

Supplementary material for “NeuPlume: Probabilistic inversion of atmospheric point-source emissions from sparse observations”

Lei Wang¹ and Xin Ma²

¹School of Earth and Space Science and Technology, Wuhan University, Wuhan 430079, China

²State Key Laboratory of Information Engineering in Surveying, Mapping and Remote Sensing, Wuhan University, Wuhan 430079, China

Correspondence: Xin Ma (maxinwhu@whu.edu.cn)

Supplementary Figure S1. Posterior Distribution for Synthetic Case 1

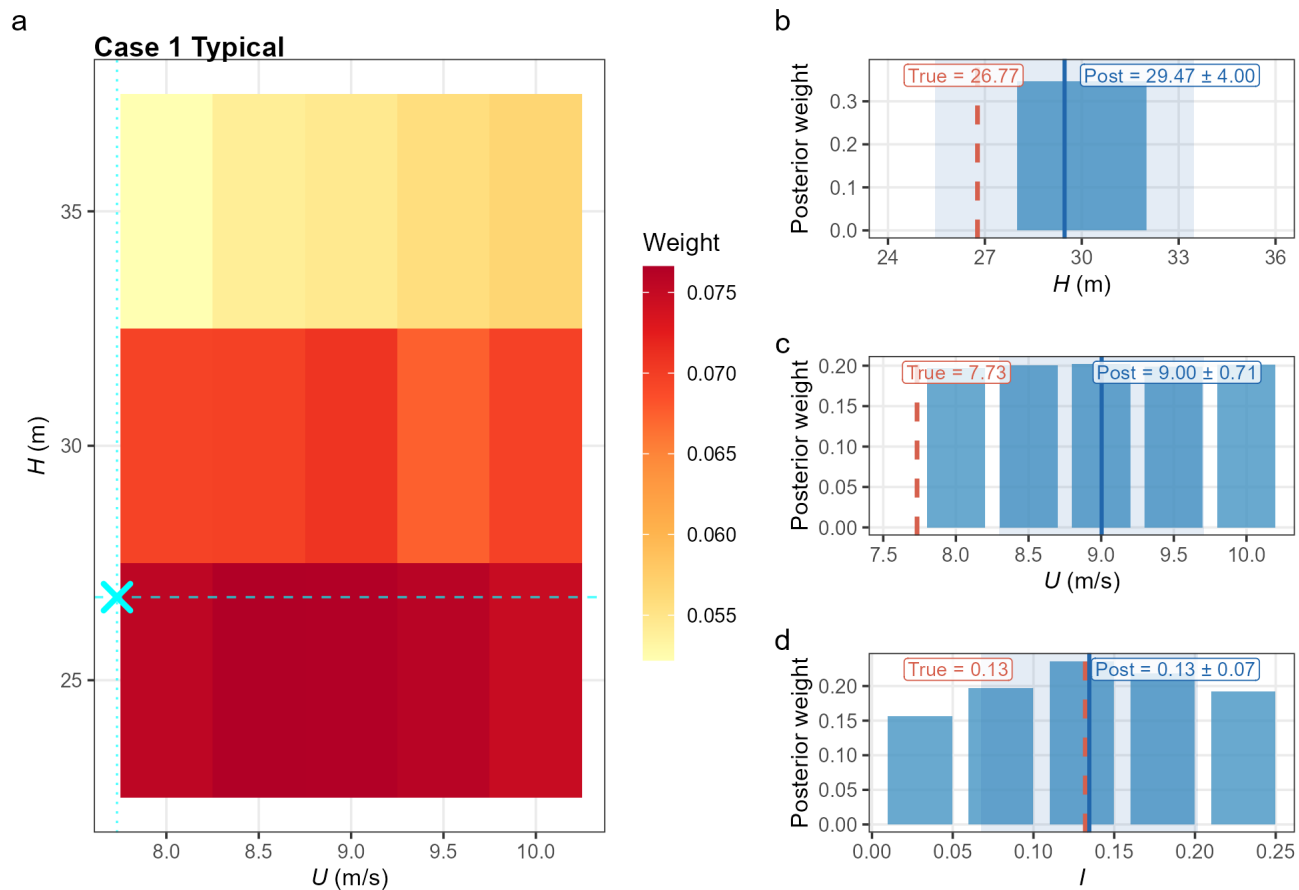


Figure S1. Complete posterior distribution for synthetic Case 1. It shows the joint density and marginal histograms of the three parameters (H , U , and I) at $\tau = 1.0$. H and U exhibit clear unimodal posteriors, indicating strong identifiability of effective release height and wind speed in this case. The marginal distribution of I is wider, indicating weaker observational constraints on turbulence intensity.

Supplementary Figure S2. Orthogonal concentration slices

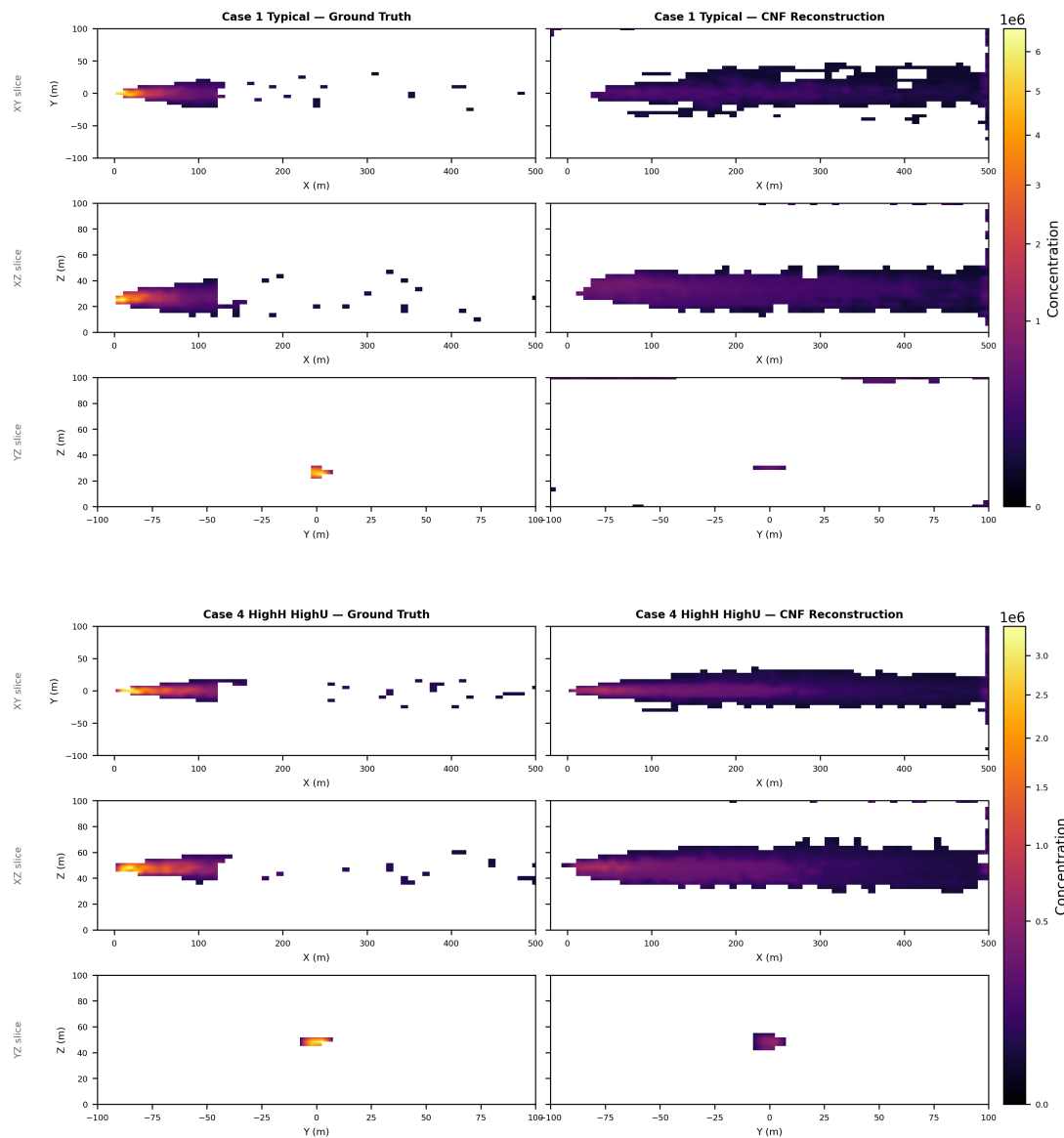


Figure S2. Orthogonal concentration slice comparison for Case 1 and Case 4. Top: ground-truth fields from the Lagrangian stochastic model; bottom: NeuPlume conditional neural field reconstructions. Rows show the xy , xz , and yz cross-sections through the plume centerline, assessing whether Hash-INR compression preserves the main plume morphology and vertical structure.

Supplementary Figure S3. 6-case parameter errors

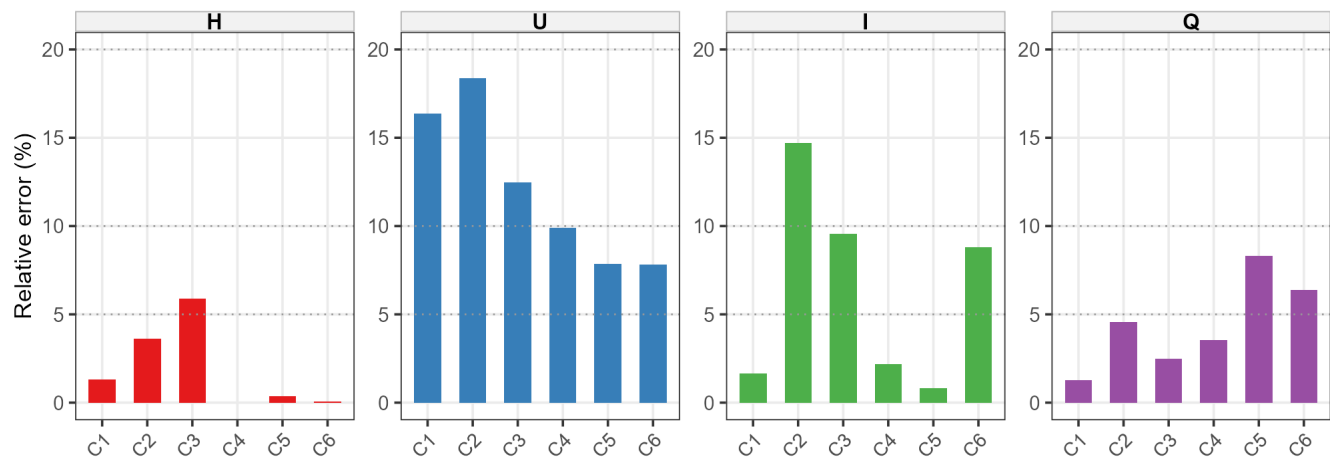


Figure S3. Per-case parameter errors for the 6 synthetic test cases under the blind-inversion protocol. The figure reports relative errors (%) for the 4 inversion parameters (Q , H , U , and I), complementing the mean-error summary in the main-text synthetic-results table.

5 Supplementary Table S1. Coarse-to-fine search ablation

Table S1. Case-wise results for the coarse-to-fine search ablation. Values are Q and H inversion errors (%) for six synthetic cases.

Case	Q error: coarse only (%)	Q error: coarse-to-fine search (%)	H error: coarse only (%)	H error: coarse-to-fine search (%)
1 – Typical case	13.7	14.2	12.1	1.1
2 – High I	34.4	10.9	12.6	1.3
3 – Low H , low U	49.9	17.3	6.1	4.8
4 – High H , high U	1.7	2.1	4.3	0.3
5 – Low U	15.0	7.3	11.6	0.5
6 – Very high I	35.4	8.2	5.1	0.6
Mean	25.0	10.0	8.6	1.4

Supplementary Table S2. Gaussian plume control experiment

Gaussian plume (GP) control on analytical GP synthetic data. GP/NeuPlume inversion errors (%) are reported; known- U GP errors are $< 0.01\%$, so the main-text synthetic-results table mainly reflects non-Gaussian plume morphology, not GP implementation error.

Table S2. Gaussian plume control experiment.

Case	GP known- U Q error (%)	GP known- U H error (%)	GP blind inversion Q error (%)	GP blind inversion U error (%)
1 – Typical	<0.01	<0.01	180	—
2 – High I	<0.01	<0.01	195	—
3 – Low H , low U	<0.01	<0.01	643	—
4 – High H , high U	<0.01	<0.01	99	—
5 – Low U	<0.01	<0.01	1991	—
6 – Very high I	<0.01	<0.01	1196	—
Mean	<0.01	<0.01	718	—

10 **Supplementary Table S3. Real-data baselines**

Table S3. Pniówek V ventilation-shaft baselines. GP and MB use the same four NeuPlume flights reported in the main-text real-data table; IG = 9.5 ± 3.5 kt/yr is the same-campaign published reference.

Flight	GP blind \hat{Q} (kt/yr)	GP blind \hat{H} (m)	GP known U \hat{Q} (kt/yr)	GP known U \hat{H} (m)	MB known U \hat{Q} (kt/yr)
#11	831	—	46	—	0.009
#12	31	—	41	—	0.013
#14	1792	—	49	—	0.055
#15	25	—	32	—	0.040

Supplementary Table S4. Boundary-loss and posterior-scope diagnostics

Table S4. Boundary-loss diagnostics for the six synthetic cases. The diagnostic uses the same LSM domain, time step, emission rate, and one wash-out cycle as the manuscript simulations.

Metric	Mean	Minimum	Maximum
Particle exit fraction	0.925	0.911	0.931
Retained particle fraction	0.075	0.069	0.089
Side/top share of exits	0.082	7.7×10^{-6}	0.207
Downwind share of exits	0.918	0.793	1.000
Side/top share of emitted particles	0.077	7.0×10^{-6}	0.192

Table S5. Posterior height-boundary and wind-scaling diagnostics for the real UAV flights. Height flags indicate posterior or MAP estimates within 5 m of the 50 m grid upper bound, including MAP values above the bound after continuous refinement.

Flight	Height-boundary flag	$\bar{U}_{blind}/U_{meteo}$	$\bar{Q}_{blind}/\bar{Q}_{known-U}$
#11	yes	0.37	0.43
#12	yes	0.36	0.51
#14	no	0.30	0.68
#15	no	2.17	3.41